Experimental analysis of crack evolution in concrete by the acoustic emission technique

J. Saliba
Université de Bordeaux, Institut de Mécanique et d'Ingénierie (I2M), Département Génie Civil et Environnemental (GCE), Talence, France
j.saliba@i2m.u-bordeaux1.fr

A. Loukili, J.P. Regoin
LUNAM Universite, UMR-CNRS 6183, Ecole Centrale de Nantes, Institut de Recherche en Génie Civil et Mécanique (GeM), Nantes, France
ahmed.loukili@ec-nantes.fr; Jean-Pierre.Regoin@ec-nantes.fr

D. Grégoire, L. Verdon, G. Pijaudier-Cabot
Université de Pau et Pays Adour, Laboratoire des Fluides Complexes et leurs Réservoirs, LFC-R UMR5150, Anglet, France
david.gregoire@univ-pau.fr; laura.verdon@univ-lorraine.fr; Gilles.Pijaudier-Cabot@univ-pau.fr

ABSTRACT. The fracture process zone (FPZ) was investigated on unnotched and notched beams with different notch depths. Three point bending tests were realized on plain concrete under crack mouth opening displacement (CMOD) control. Crack growth was monitored by applying the acoustic emission (AE) technique. In order to improve our understanding of the FPZ, the width and length of the FPZ were followed based on the AE source locations maps and several AE parameters were studied during the entire loading process. The b-value analysis, defined as the log-linear slope of the frequency-magnitude distribution of acoustic emissions, was also carried out to describe quantitatively the influence of the relative notch depth on the fracture process. The results show that the number of AE hits increased with the decrease of the relative notch depth and an important AE energy dissipation was observed at the crack initiation in unnotched beams. In addition, the relative notch depth influenced the AE characteristics, the process of crack propagation, and the brittleness of concrete.

KEYWORDS. Concrete; Crack; Acoustic Emission technique; Notch depth; Unnotched beams.

INTRODUCTION

Fracture of concrete is accompanied by the formation and evolution of an inelastic zone, referred to as the fracture process zone (FPZ), around the propagating crack tip. The existence of the FPZ is responsible of the nonlinear behaviour of concrete and lead to complex phenomena as size effects. In fact, the length and the width of the FPZ

are strongly influenced by the dimensions of specimens/structures. Many researchers tried to characterize the FPZ and its evolution during crack extension in order to obtain size independent fracture parameters for the application of fracture mechanics of concrete. For Hillerborg [1], the length of the FPZ was related to the length of cohesive zone or the characteristic length which is a pure property of the materials, while Bazant & al. [2, 3] modeled the FPZ as a band with a fixed width related to the size of aggregates in concrete.
Recently, various experimental methods were employed to detect the fracture process as the holographic interferometry, the dye penetration, the scanning electron microscopy, the X-rays, the digital image correlation, etc. However, these methods offer either the images of the material surface to observe micro-features of the concrete with qualitative analysis, or the black-white fringe patterns of deformation on the specimen surface (except for 3D tomography), from which it is difficult to observe profiles of the cracked material. In this study, the growth of the fracture zone is investigated using the AE technique. This later allows a continuous and a real time data acquisition, and thus the damage evolution during loading tests can be recorded. The AE technique is a passive method that has been proved to be very effective to locate microcracks and to study different failure modes in concrete structure [4-7]. It presents a large potential of applications and has been used in the past to study the influence of different parameters on FPZ, such as the effect of aggregates [8, 9], porosity [10], creep [11, 12], notch depth [13], specimen geometry and type of loading [14]. The damage is then evaluated based on statistical analysis and measurement of AE activity [15] or on quantitative and signal based techniques (moment tensors) [7].
The objective of this paper is to characterize the FPZ and its evolution during the fracture process in unnotched and notched concrete beams with different notch depths based on the AE technique. First, material and experimental methods are presented. Secondly, fracture measurements are analyzed and the characterization of crack evolution at different loading stages is suggested with AE technique. Finally, the effect of the notch to depth ratio on fracture growth is described based on the experimental observations.

EXPERIMENTAL PROCEDURE

Materials and specimens

The experiments are realised by Grégoire & al. and reported in [16, 17]. In this study, only the comparison between notched and unnotched beams was realised. The tests realised on notched beams were conducted on beams with a constant depth of 200 mm and length of 700 mm with an effective span equal to 500 mm. Two notch to depth ratio of 0.2 and 0.5 were considered and labeled respectively SN200, LN200. While tests realised on unnotched beams were conducted on beams with the same dimensions as earlier labeled UN200 and on beams with a depth of 100 mm, a length of 350 mm and an effective span equal to 250 mm labeled UN100. The thickness was kept constant for all the beams at 50 mm.
Tests were conducted under closed-loop crack mouth opening displacement (CMOD) control. The CMOD measurement consists in recording the distance between two alumina plates glued on the bottom surface of the beam, on each side of the initial notch. For unnotched beams, the alumina plates were glued at a distance from midspan equal to half the depth of the beam (details may be found in [16]).

Acoustic emission technique

The AE system comprised of an eight channel AEwin system, a general-purpose interface bus (PCI-DISP4) and a PC for data storage analysis. A 2D analysis with an AEwin algorithm is performed for the localization of AE events. For the source to be located in 2D, a wave must reach at least three sensors. In this study, 4 piezoelectric sensors with a frequency of 50-200 kHz and a resonance frequency of 150 kHz were used. The transducers were placed around the expected location of the FPZ to minimize errors in the AE event localization. They were placed on the specimen with silicon grease as the coupling agent. The sensors form a rectangular grid location on one side of (75 x120 mm^2) for UN200 beams, (60 x120 mm^2) for UN100 beams, (105 x 120 mm^2) for SN200 beams and (110 x 120 mm^2) for LN200 beams [17] (Fig. 1).
The detected signals were amplified with a 40 dB gain differential amplifier. The recorded AE amplitudes ranged from 0 to 100 dB. In order to overcome the background noise, the signal detection threshold was set at a value of 35 dB slightly above the background noise. The acquisition system was calibrated before each test using a pencil lead break procedure HSU-NIELSEN [18]. Location accuracy is measured in the range of 5 mm by applying the pencil lead fracture at a known location of the specimen. The measured effective velocity is equal to 3800 m/s. Each waveform was digitized and stored and signal descriptors such as rise time, counts, energy, duration, amplitude, average frequency and counts to peak were captured and calculated by AEwin system.

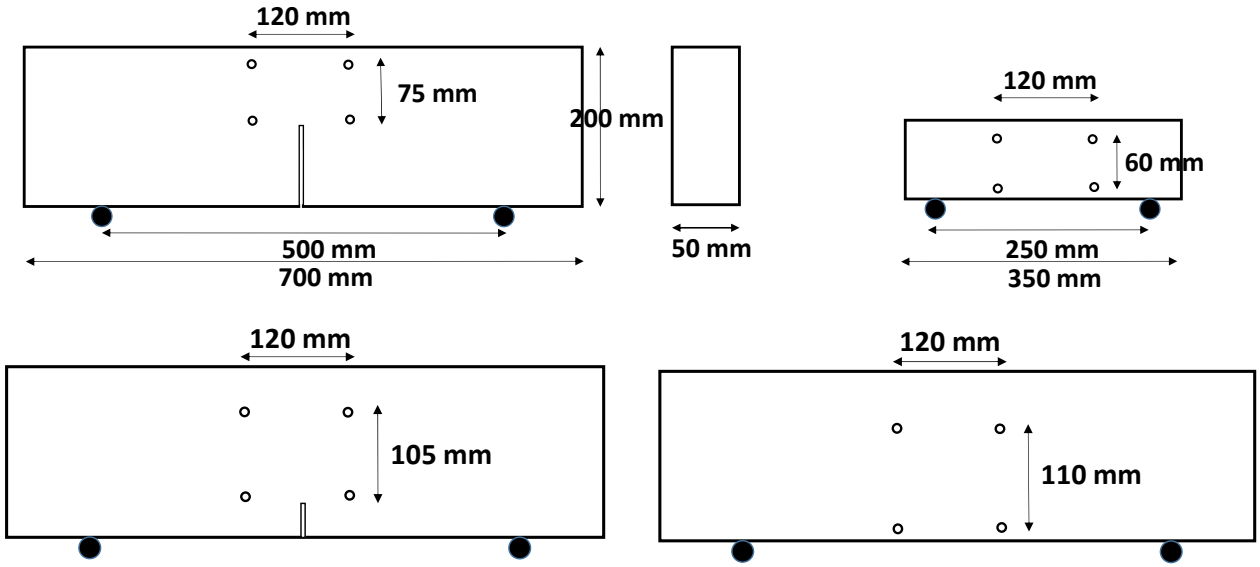

Figure 1: Specimen geometry and AE transducers position for LN200, UN100, SN200 and UN200beams.

EFFECT OF RELATIVE NOTCH DEPTH ON AE CHARACTERISTIC

The load-CMOD curves of notched and unnotched concrete beams are shown in Fig. 2 (a). Damage quantification was calculated based on the AE activity represented by the cumulative number of AE hits (Fig.2 (b)). For the beams with a depth of 200 mm, the results show that as the notch depth decreases, the total number of AE hits increases requiring higher energy for overcoming interfacial bond along the ligament length. For UN100, the rate of AE hits is similar to that of UN200 beams at the beginning and reaches later values between the total number of AE hits for LN200 (presenting the same ligament length) and the total number of AE hits for UN200 which could be related to the additional energy required for the crack initiation in unnotched beams and to different crack lengths. The cumulated AE energy followed the same trend and gives information on the cracks initiation that progress until the failure and thus could be related to the fracture energy measured on a global scale.

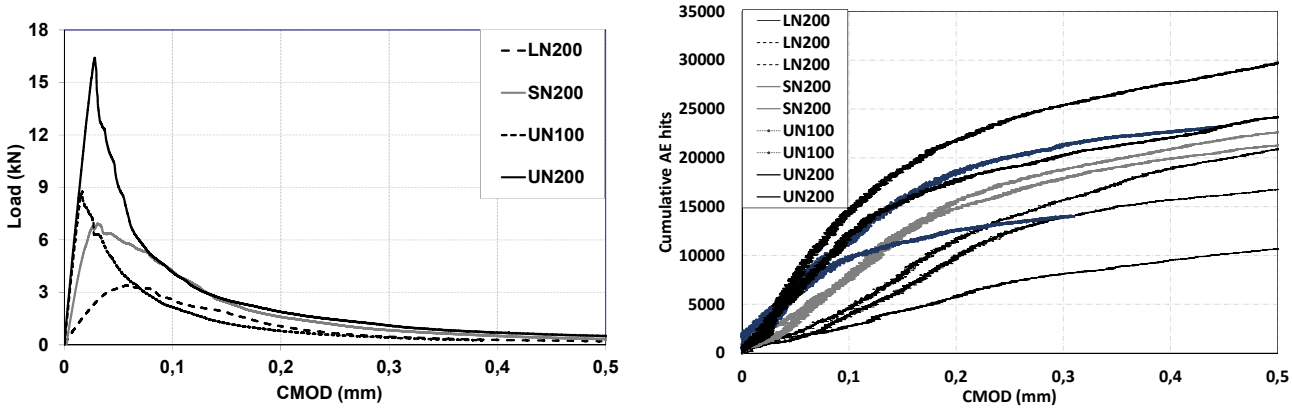

Figure 2: a) Load-CMOD curves and b) cumulative AE hits in function of CMOD for UN200, UN100, SN200 and LN200 beams.

Fig. 3 presents the correlation between the load-CMOD curves and the AE characteristics during the entire loading process for the beams. The AE activity is in good correlation with the load CMOD curves. The rate of AE hits is low at the beginning and then increases after the load reached the peak indicating the propagation of the crack. The results show that the relative notch depth had a great effect on AE characteristics. In the ascending branch of load CMOD curve, the AE hits distribution increases slowly for notched beams. As the load reached about 80% of the maximal strength the rate of AE hits increases and then decreases in the post peak region at 50% of the maximal strength in the post peak region

for SN200 and at 20% for LN200. The position of the peak of occurring AE hits changed also with the relative notch depth and shifted to the latter part of the descending branch as the relative notch depth decreased.
For unnotched beams, the peak appeared earlier with a more important peak magnitude however the width of the occurring AE hits distribution peak is less important and the decrease of AE hits distribution becomes steeper in the descending branch following the same trend of the load-CMOD curves. This behavior indicate a more brittle behavior for unnotched concrete beams.
For UN100 beams, the AE distribution presents a peak near the maximal strength with a larger width and shows an intermediate behavior between UN200 and notched beams. This indicates a more ductile behavior for UN100 beams in comparison with UN200 beams and thus a similar influence of the notch depth and specimen's depth on fracture process after the initiation of the crack.

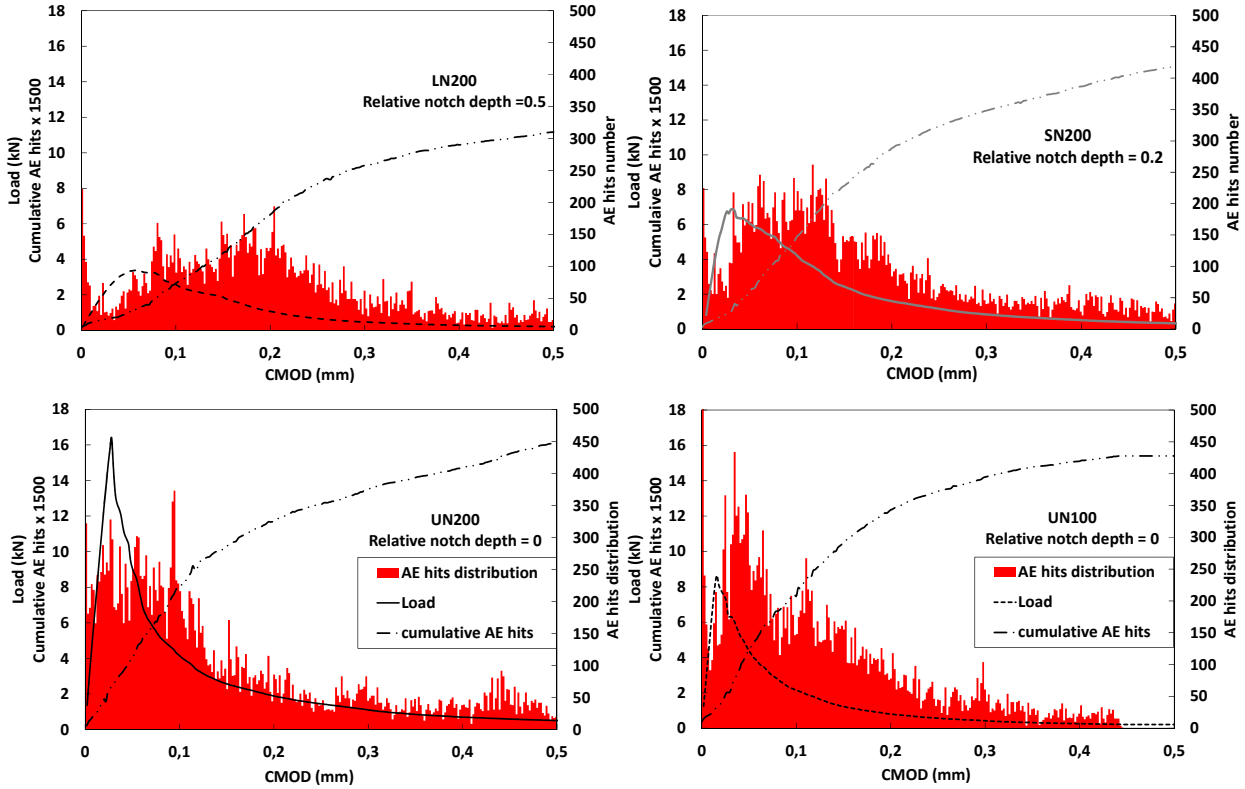

Figure 3: Correlation of load vs. CMOD curves with the AE characteristic in UN200, UN100, SN200 and LN200 beams.

DAMAGE LOCALIZATION

During the formation of a crack, energy is emitted as an elastic wave and propagates from the crack location to the AE transducers at specimen surface. The localization map of AE events is based on arrival times of the first wave at each transducer and their respective velocity in concrete specimen. Once the arrival time is picked, least-square method is used to estimate the event location. The cumulative acoustic events are placed in 2D. The detected AE events of notched and unnotched beams are presented over a window covering the specimen height and a width of 300 mm centered at the notch (Fig. 4). The localization maps of AE sources are drawn at the peak, at 50% of the maximal strength in the post-peak region and at the end of the rupture test. Each plotted point indicates a detected AE source. In addition to number of AE events, it is important to investigate AE signal parameters. The initiation and propagation of cracks in concrete are generally correlated to AE signals amplitude. Extensive studies have shown that the absolute acoustic energy is also an important parameter to characterize an event [19]. Thus, the 2D localization maps of AE events are classified in terms of their levels of energy. Six energy levels are defined. It can be seen that AE events of higher energy levels are located in the core of the FPZ [4] indicating the crack path with a rough and complex fracture surface inside the specimen.

At the peak load, the localization maps show that the AE events appeared first for LN200 beams, then SN200, UN100 and UN200 respectively. The localization maps at 50% in the post peak region show also different crack evolution with a more important crack length for notched beams. For unnotched beams, the localization of AE events begins earlier for UN100 then UN200 with a more important crack length indicating also a more ductile behavior for small beams due to different stress gradient along the ligament length. A crack branching was also observed in the localization maps of UN200 and SN200 which could be due to an aggregate interlock.

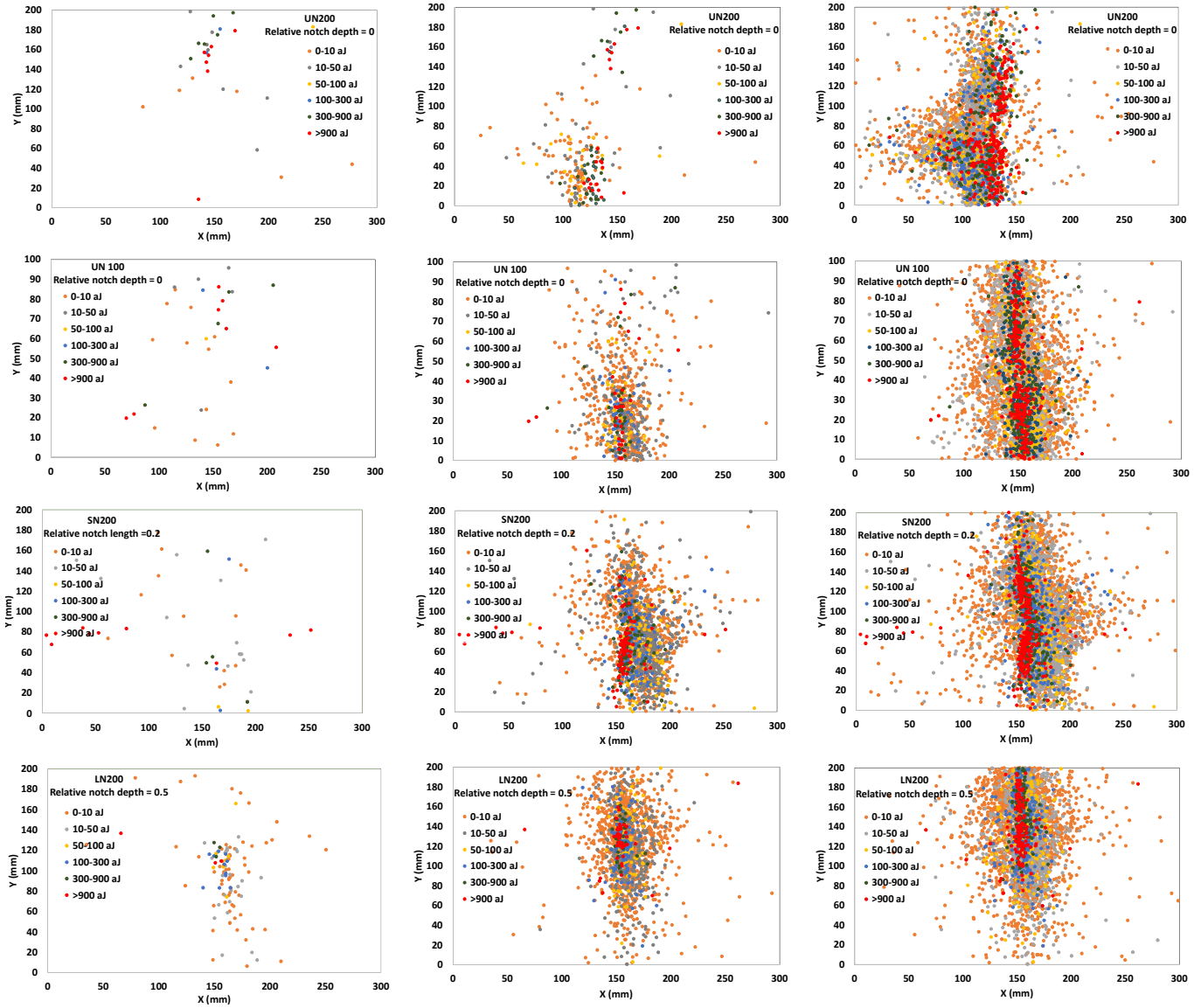

Figure 4: Localization maps of the AE events at the peak, at 50% of the maximal strength in the post-peak region and at the end of the rupture test for UN200, UN100, SN200 and LN200 beams.

CHARACTERIZATION OF THE FPZ

Different approaches were proposed to determine the length of the FPZ based on the AE technique. Lertsrisakulrat et al. [20] and Watanabe et al. [21] proposed different simplified empirical relations for the localized compressive fracture length. They considered that the length of the FPZ is equal to the zone where the local energy is superior to 15% of the total energy in the specimens or the region where the distribution of peak amplitude or AE energy is superior to 30% as the AE criterion to distinguish the failure zone. The length and the width of damage

zone were also computed using probability and statistics laws by dividing the damage zone into two areas: the zone of confidence with high damage and a weak damage zone based on the distribution either of the number or the amplitude of acoustic emission events [15].

In our study, the length of the FPZ was estimated based on AE events density along the ligament length. Fig. 5(a) shows the density of AE events at each Y location at 10% of the maximal strength in the post-peak region for UN200, UN100, SN200 and LN200 beams. For notched beams, it can be seen that ahead of the notch tip, the number of AE events increases progressively due to the front boundary, attains the maximum value (N_{max}) and then remains almost constant for some distance along the ligament length and decreases as the crack propagates towards the back boundary. The same behavior can be observed with the AE energy distribution. The curves clearly follow the energy dissipation trend shown by the boundary effect model. The fracture energy through the front and back boundary effect can be taken into account by assuming a trilinear variation of local fracture energy over the ligament length [22, 23, 24, 25, 26]. However for unnotched beams, the AE events density presents an important peak near the front boundary indicating a more important energy dissipation for crack initiation, then decreases along the ligament length.

The occurrence of AE events can be considered as a criterion to follow the crack propagation through the beam depth for different loading levels. Therefore, the length of the FPZ was defined as the length of the segment from notch tip to the intersection of the histogram with the horizontal line located at 20% of N_{max}. Fracture examination in concrete through combined techniques as digital image correlation and X-rays can give additional information; however the monitoring of the evolution of the fracture length with AE technique shows similar trends as those later and proved to be quantitatively acceptable [4, 27]. The relative fracture length (Lcrack/D), i.e. the ratio of length of fracture from the crack mouth (Lcrack) to height of specimen (D), obtained with the AE technique at different loading intervals is plotted in Fig. 5 (b) for UN200, UN100, SN200 and LN200 specimens. .

For the LN200 beams, fracture initiates earlier at 90% of the maximal strength in the pre-peak regime followed by SN200, while the fracture growth of unnotched beams starts after the peak load. The relative fracture length in LN200 specimen is more important in comparison with SN200, UN100 and UN200 and the relative fracture length of UN100 has values between that of UN200 and SN200 beams. The fracture growth is relatively abrupt at the beginning and decreased at the end. A similar behavior was also observed while studying size effect with a more important crack length for smaller beams [27]. Note here that the AE analysis does not give precise information about the tip of the stress free crack because the criteria used for determining the length of the FPZ may cause a loss of information as it is not possible to know exactly the crack tip position.

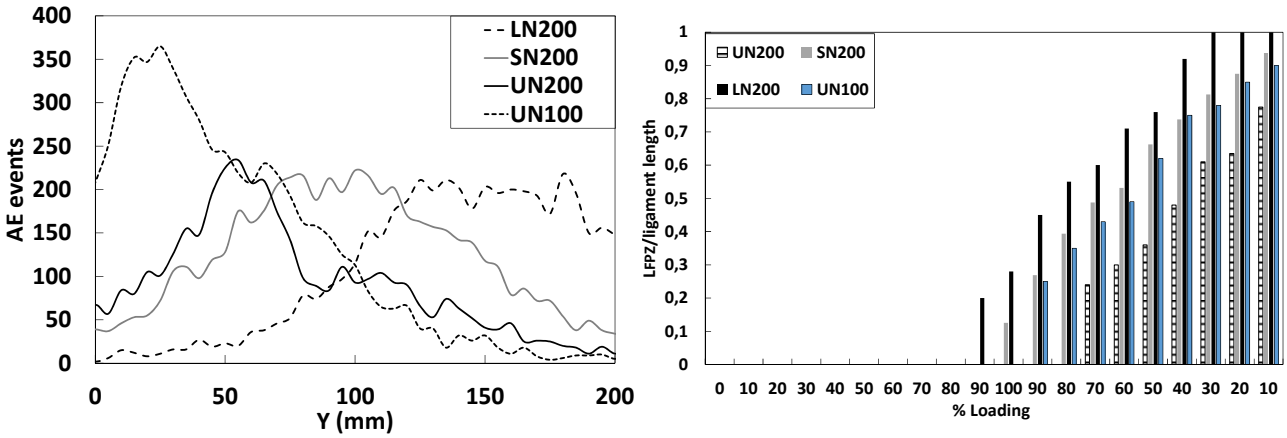

Figure 5: a) Cumulative AE events at each Y location and b) evolution of relative crack length with load steps for UN200, UN100, SN200 and LN200 beams.

Based on the localization maps, the width of the FPZ was also estimated based on the horizontal line located at 20% of N_{max} which separate the zone with a high number of events representing the localization of microcracking and the outside zone where the level of damage is lower [15] (Fig. 6). The discrepancy between the widths of the FPZ is relatively important, this could be due to different sources of error: the localization of AE events is realized in 2D on one face of the specimen however the crack path inside the thickness of the beams is different (3D) due to the internal heterogeneity of the material. In addition, the crack path is dominated by the distribution of aggregates and other softening mechanisms and the width of the FPZ cannot be determined correctly when main crack branches into microcracks in multiple directions. However, the results show that the width of FPZ tend to increase with the decrease of the relative notch depth. This behavior was also observed in Otsuka and al. [4]

Those differences in the length and the width of the FPZ show a non-uniform stress distribution in the cross section of the beams with different sizes and different relative notch depth which could be responsible, in combination with the softening behavior of concrete, of the size effect in concrete structures.

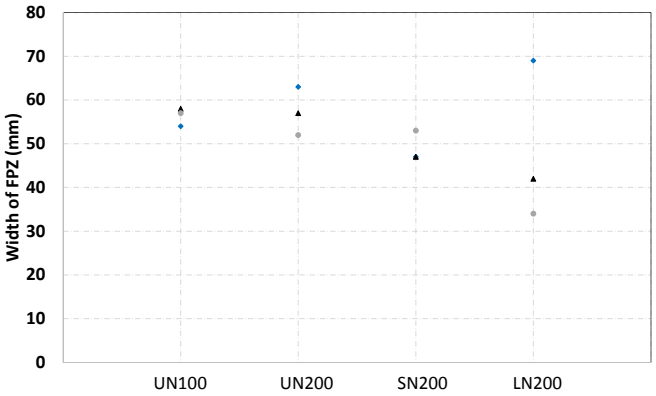

Figure 6: The width of the FPZ for UN200, UN100, SN200 and LN200 beams

THE AE BASED IB-VALUE

The AE peak amplitude is related to the magnitude of cracks developed during fracture. Micro-cracks generate an important number of small AE hits amplitude, while macro-cracks generate few hits with higher amplitude. To determine the overall fracture quantitatively on basis of peak amplitude, the b-value originated from seismology is performed. It is defined as the absolute value of the slope of the cumulative distribution of AE hits amplitude. If small-scale fractures are superior to large-scale fractures, the Ib-value tend to increase, in the contrary if large-scale fractures are superior to small-scale fractures, the Ib-value tends to decrease. The Ib-value was calculated using the peak amplitudes of 50 successive hits as:

$$Ib = \frac{\log_{10} N(\mu - \alpha_1 \sigma) - \log_{10} N(\mu + \alpha_2 \sigma)}{(\alpha_1 + \alpha_2)\sigma}$$

where σ is the standard deviation of the amplitude distribution, μ is the mean value of the amplitude distribution, α_1 is the coefficient related to the smaller amplitude and α_2 is the coefficient related to the fracture level. α_1 and α_2 are constants and are equal to 0 and 1 respectively. Fig. 7 shows the evolution of the improved Ib-value. The results show that Ib-value decreases near the peak and then fluctuates strongly in the post peak region. Thus small-scale fracturing with higher frequencies were dominantly generated up to the peak then large scale fractures with lower frequency started near the peak and continue to occur.

CONCLUSION

An experimental study is presented in order to monitor fracture growth during three point bending tests in notched and unnotched concrete beams. The AE technique was also employed to follow the damage evolution and to characterize the FPZ. The global mechanical response of the beams can be then translated from the local fracture process in the material. The total number of the released AE hits and AE energy increases with the decrease of the relative notch depth. In addition, the correlation between the load–CMOD curves and AE analysis shows that as the notch depth increases the peak of AE records becomes lower and wider, and moves along the horizontal axis indicating a more ductile behavior. The fracture process zone length was also monitored with AE technique. The evolution of the fracture length was highly dependent on the relative notch depth. The initiation of the fracture is detected earlier in notched beams compared to unnotched beams with a higher relative crack length respectively. An additional energy dissipation for crack initiation was also observed in unnotched beams.

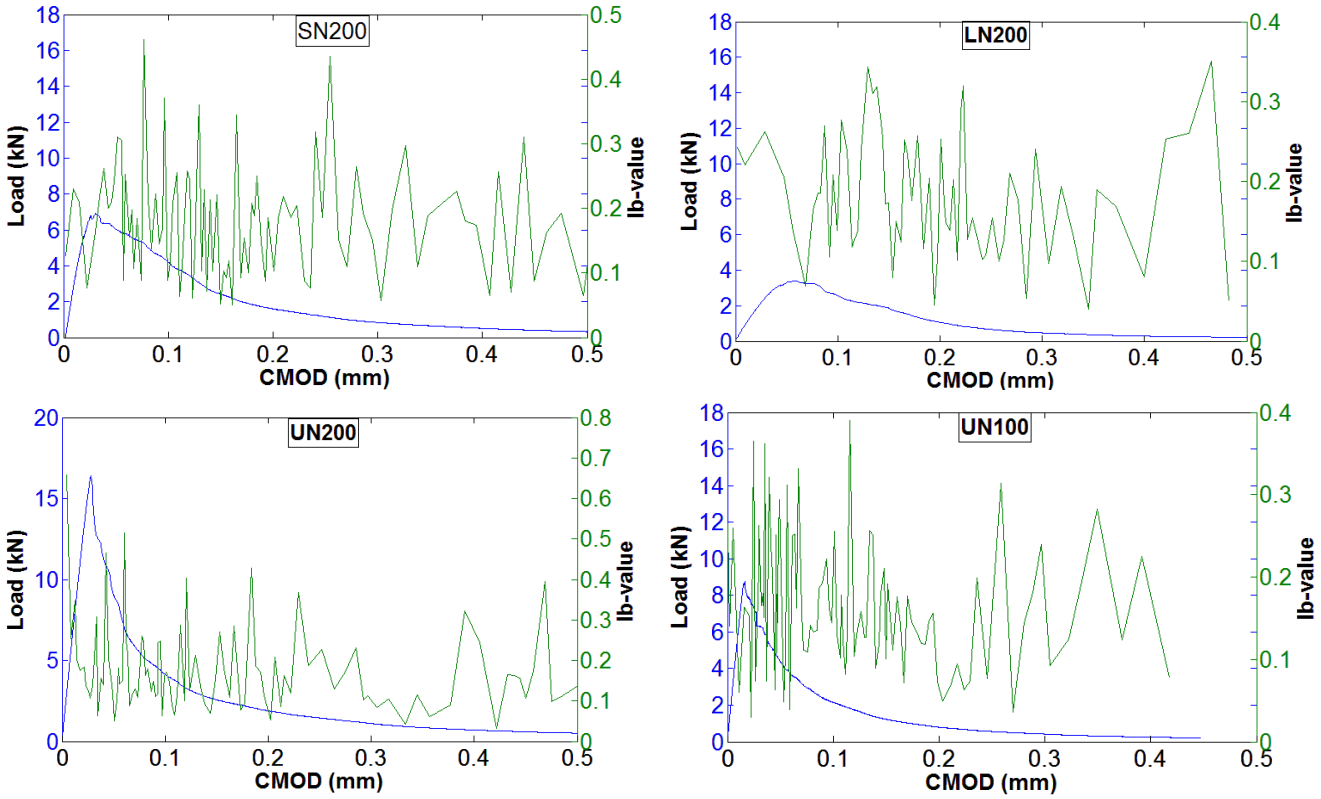

Figure 7: Load and Ib-value versus CMOD for UN200, UN100, SN200 and LN200 beams.

REFERENCES

[1] Hillerborg, A., Modéer, M., Petersson, P. E., Analysis of crack formation and crack growth in concrete by means of fracture mechanics and finite elements, Cement Concrete Research, 6 (1976) 773–782.
[2] Bazant, Z.P., Ohh, B., Crack band theory for fracture of concrete, Materials and Structures, 16 (1983) 155-177.
[3] Bazant, Z.P., Size effect in blunt fracture: Concrete, rock, metal, Journal of Engineering Mechanics (ASCE), 110 (1984) 518–535.
[4] Otsuka, K., Date, H., Fracture process zone in concrete tension specimen, Engineering Fracture Mechanics, 65 (2000) 111-131.
[5] Landis, E.N., Shah, S.P., The influence of microcracking on the mechanical behaviour of cement based materials, Cement Based Materials, 2 (1995) 105-118.
[6] Chen, B., Liu, J., Experimental study on AE characteristics of three-point-bending concrete beams, Cement and Concrete Research, 34 (2004) 391-397.
[7] Grosse, C.U., Fink, F., Quantitative evaluation of fracture processes in concrete using signal-based acoustic emission techniques, Cement & concrete composites, 28 (2006) 330-336.
[8] Wu, K., Chen, B., Yao, W., Study of the influence of aggregate size distribution on mechanical properties of concrete by acoustic emission technique, Cement & Concrete Research, 31 (2001) 919-923.
[9] Chen, B., Liu, J., Effect of aggregate on the fracture behavior of high strength concrete, Construction and Building Materials, 18 (2004) 585-590.
[10] Haidar, K., Pijaudier-Cabot, G., Dubé, J.F., Loukili, A., Correlation between the internal length, the fracture process zone and size effect in model materials, Materials and Structures, 38 (2005) 201–210.
[11] Saliba, J., Loukili, A., Grondin, F., Regoin, J.-P., Influence of basic creep on cracking of concrete shown by the Acoustic Emission technique, Materials and Structures, 45 (2012) 1389-1401.

[12] Saliba, J., Loukili, A., Grondin, F., Regoin, J.-P., Identification of damage mechanisms in concrete under high level creep by the acoustic emission technique, Materials and structures, 47 (2014) 1041-1053.
[13] Zhang, D., Wu, K., Fracture process zone of notched three-point bending concrete beams, Cement and Concrete Research, 29 (1999) 1887-1892.
[14] Labuz, J.F., Cattaneo, S., Chen, L., Acoustic emission at failure in quasi-brittle materials, Construction and building Materials, 15 (2001) 225-233.
[15] Hadjab, H.S., Thimus, J.F., Chabaat, M., The use of acoustic emission to investigate fracture process zone in notched concrete beams, Current Science, 93 (2007) 648-653.
[16] Grégoire, D., Rojas-Solano, L.B., Pijaudier-Cabot, G., Failure and size effect for notched and unnotched concrete beams. International Journal of Numerical and Analytical Methods in Geomechanics, 37 (2013) 1434-1452.
[17] Grégoire, D., Verdon, L., Lefort, V., Grassl, P., Saliba, J., Regoin, J.P., Loukili, A., Pijaudier-Cabot, G., Mesoscale analysis of failure in quasi-brittle materials: comparison between lattice model and acoustic emission data, International Journal of Numerical and Analytical Methods in Geomechanics, (2015), DOI 10.1002.nag.2363.
[18] RILEM TC212-ACD recommendation, Acoustic emission and related NDE techniques for crack detection and damage evaluation in concrete, Materials and Structures, 43 (2010) 1177-1181.
[19] Muralidhara, S., Raghu Prasad, B.K., Eskandari, H., Karihaloo, B., Fracture process zone size and true fracture energy of concrete using acoustic emission, Construction and Building Materials, 24 (2010) 479-486.
[20] Lertsrisakulrat, T., Watanabe, K., Matsuo, M., Niwa, J., Experimental study on parameters in localization of concrete subjected to compression, J.Materials Conc. Struc., Pavements, JSCE, 50 (2001) 309-321.
[21] Watanabe, K., Niwa, J., Iwanami, M., Yokota, H., Localized failure of concrete in compression identified by AE method, Construction and Building Materials, 18 (2003) 189-196.
[22] Karihaloo, BL, Abdalla, HM, Imjai, T., A simple method for determining the true specific fracture energy of concrete, Mag Concrete Research, 55 (2003) 471–481.
[23] Duan, K, Hu, X, Wittmann, F.H., Boundary effect on concrete fracture and non-constant fracture energy distribution, Engineering Fracture Mechanics, 70 (2003) 2257–2268.
[24] Hu, X, Duan, K., Influence of fracture process zone height on fracture energy of concrete, Cement Concrete Research, 34 (2004) 1321–1330.
[25] Duan, K, Hu, X, Wittmann, F.H., Size effect on specific fracture energy of concrete, Engineering Fracture Mechanics, 74 (2007) 87–96.
[26] Muralidhara, S., Raghu Prasad, B.K., Karihaloo, B.L., Singh, R.K., Size-independent fracture energy in plain concrete beams using tri-linear model, Construction and Building Materials, 25 (2011) 3051-3058.
[27] Alam, S.Y., Saliba, J., Loukili, A., Fracture examination in concrete through combined digital image correlation and acoustic emission techniques, Construction and Building Materials, 69 (2014) 232–242.